

Heterobinucleating Ligand-Induced Structural and Chemical Variations in [(L)Fe^{III}-O-Cu^{II}]⁺ μ -Oxo Complexes

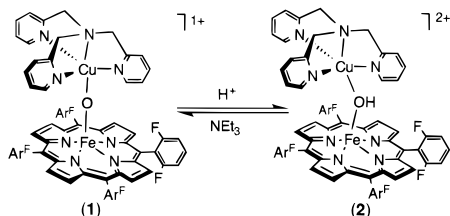
Honorio V. Obias,[†] Gino P. F. van Strijdonck,[†]
Dong-Heon Lee,[†] Martina Ralle,[‡] Ninian J. Blackburn,[‡] and
Kenneth D. Karlin^{*,†}

Department of Chemistry, The Johns Hopkins University
Baltimore, Maryland 21218, and Department of Chemistry,
Biochemistry, and Molecular Biology
Oregon Graduate Institute of Science & Technology
Portland, Oregon 97291-1000

Received April 2, 1998

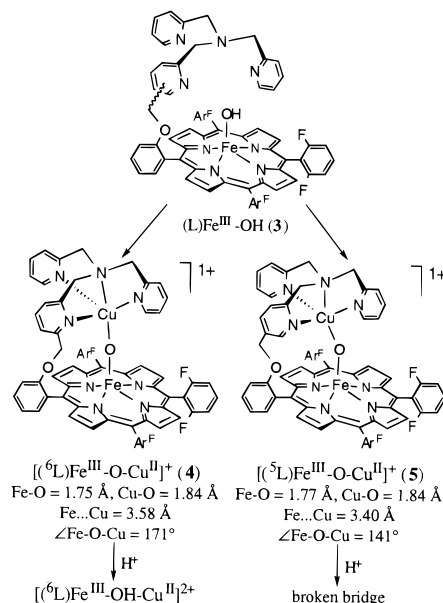
The study of (porphyrinate)Fe^{III}•••Cu complexes¹ is of current interest in modeling structural and functional aspects of the binuclear active center in the heme-copper oxidase enzyme superfamily, the cytochrome *c* and quinol oxidases. At the heme a₃-Cu_B active site, dioxygen binds and undergoes 4e⁻/4H⁺ reduction to water. This chemistry is directly coupled to proton translocation through these membrane-spanning proteins; the electrochemical gradient thereby generated is used to drive ATP synthesis.² Recent cytochrome *c* oxidase (CcO) X-ray diffraction studies^{3–5} have helped to clarify aspects of structure and function. However, in addition to questions about intermediates in the O₂-reduction process^{2–6} and the possible proton and/or electron-transfer role of histidine (or nearby tyrosine) Cu_B ligands,^{4,5,7} important issues related to ligand-binding properties and the nature of Fe(III)-X-Cu(II) species (X = possible bridging ligand) exist. For example, protein X-ray data⁵ suggest that (hydro)peroxide and azide (and even CO, in the reduced enzyme) bridge the Fe and Cu ions.

Our own investigations have included the characterization of the μ -oxo complex, [(F₈-TPP)Fe^{III}-O-Cu^{II}(TMPA)]⁺ (**1**),⁸ and



its conjugate acid, [(F₈-TPP)Fe^{III}-OH-Cu^{II}(TMPA)]²⁺ (**2**).⁹ We have suggested^{9b} a μ -OH⁻ complex like **2** as a possible resting-state candidate; a μ -O²⁻ or a μ -OH⁻ species may also be considered as a possible intermediate occurring during enzyme turn-

Scheme 1



over, as an O-O cleavage product which induces proton transfer as part of the enzyme function.⁷ Here, we describe μ -oxo compounds generated with new binucleating ligands ⁶L and ⁵L,^{10,11} which possess the TMPA moiety covalently tethered to the porphyrin periphery. The two isomeric ligands confer dramatically altered structures to the derived μ -oxo complexes **4** and **5** (Scheme 1), while also causing pronounced effects upon their spectroscopic properties and, as potentially relevant to CcO, their protonation chemistry.

We previously^{10b} described a heme/non-heme diiron μ -oxo complex using ⁵L, [(⁵L)Fe^{III}-O-Fe^{III}-Cl]⁺, from which the iron in the TMPA tether can be selectively removed, yielding a high-spin Fe^{III}-OH complex with an empty tether, (⁵L)Fe^{III}-OH (**3b**). The isomer using ⁶L, [(⁶L)Fe^{III}-OH] (**3a**), can be similarly formed.¹¹ To these complexes, addition of copper(II)-triflate and base, followed by counterion exchange (ClO₄⁻ or BARF⁻), yields the μ -oxo analogues [(⁶L)Fe^{III}-O-Cu^{II}]⁺ (**4**) and [(⁵L)Fe^{III}-O-Cu^{II}]⁺ (**5**) (Scheme 1).¹¹ These possess features similar to **1**, i.e., distinctive red-shifted Soret bands at ~435 nm, and ¹H NMR spectra with dramatically upfield-shifted Cu-ligand resonances, indicative (as for **1**)^{9c} of an S = 2 system with high-spin Fe(III) antiferromagnetically coupled to Cu(II) {**4**, 5.0 μ_B ; **5**, 4.9 μ_B (Evans method, rt)}. The spectrum for **4** (Figure 1) and that for **5**¹² reveals the lowered symmetry imposed by the ligand tether.¹³

Structural insights (e.g., metal-ligand, Fe•••Cu distances and \angle Fe-O-Cu values) have been obtained using EXAFS spec-

[†] Johns Hopkins University.

[‡] Oregon Graduate Institute.

* Author for correspondence.

(1) Kopf, M.-A.; Karlin, K. D. In *Biomimetic Oxidations*; B. Meunier, Ed.; Imperial College Press: London, 1998; Chapter 7, in press.

(2) Ferguson-Miller, S.; Babcock, G. T. *Chem. Rev.* **1996**, *96*, 2889–2907.

(3) (a) Tsukihara, T.; Aoyama, H.; Yamashita, E.; Tomizaki, T.; Yamaguchi, H.; Shinzawa-Itoh, K.; Nakashima, R.; Yaono, R.; Yoshikawa, S. *Science* **1995**, *269*, 1069–1074. (b) Tsukihara, T.; Aoyama, H.; Yamashita, E.; Tomizaki, T.; Yamaguchi, H.; Shinzawa-Itoh, K.; Nakashima, R.; Yaono, R.; Yoshikawa, S. *Science* **1996**, *272*, 1136–1144.

(4) (a) Iwata, S.; Ostermeier, C.; Ludwig, B.; Michel, H. *Nature* **1995**, *376*, 660–669. (b) Ostermeier, C.; Harrenga, A.; Ermiler, U.; Michel, H. *Proc. Natl. Acad. Sci. U.S.A.* **1997**, *94*, 10547–10553.

(5) Yoshikawa, S.; Shinzawa-Itoh, K.; Nakashima, R.; Yaono, R.; Yamashita, E.; Inoue, N.; Yao, M.; Fei, M. J.; Peters Libeu, C.; Mizushima, T.; Yamaguchi, H.; Tomizaki, T.; Tsukihara, T. *Science* **1998**, *280*, 1723–1729.

(6) Kitagawa, T.; Ogura, T. *Prog. Inorg. Chem.* **1997**, *45*, 431–479.

(7) (a) Morgan, J. E.; Verkховsky, M. I.; Wikström, M. *J. Bioenerg. Biomembr.* **1994**, *26*, 599–608. (b) Wikström, M.; Morgan, J. E.; Verkховsky, M. I. *J. Bioenerg. Biomembr.* **1998**, *30*, 139–145.

(8) Abbreviations used: F₈-TPP, tetrakis(2,6-difluorophenyl)porphyrinate; TMPA, tris(2-pyridylmethyl)amine; EXAFS, extended X-ray absorption fine structure; BARF, tetrakis(3,5-bis-trifluoromethylphenyl)borate.

(9) (a) Karlin, K. D.; Nanthakumar, A.; Fox, S.; Murthy, N. N.; Ravi, N.; Huynh, B. H.; Orosz, R. D.; Day, E. P. *J. Am. Chem. Soc.* **1994**, *116*, 4753–4763. (b) Fox, S.; Nanthakumar, A.; Wikström, M.; Karlin, K. D.; Blackburn, N. J. *J. Am. Chem. Soc.* **1996**, *118*, 24–34. (c) Nanthakumar, A.; Fox, S.; Murthy, N. N.; Karlin, K. D. *J. Am. Chem. Soc.* **1997**, *119*, 3898–3906 and references therein.

(10) (a) Karlin, K. D.; Fox, S.; Nanthakumar, A.; Murthy, N. N.; Wei, N.; Obias, H. V.; Martens, C. F. *Pure Appl. Chem.* **1995**, *67*, 289–296. (b) Martens, C. F.; Murthy, N. N.; Obias, H. V.; Karlin, K. D. *Chem. Commun.* **1996**, 629–630.

(11) See Supporting Information.

(12) Unpublished results.

(13) The pyrrole resonances (64–69 ppm) now appear as four peaks, while the methylene hydrogens on the TMPA ligand are split into a 2:1 ratio since one of the three pyridine rings is connected to the peripheral porphyrin aryl group. In **4**, selective deuteration and ²H NMR spectroscopy (Supporting Information), including the methylene-CH₂- protons on the pyridine linked to the porphyrin (at +5 ppm) confirms their assignment of -123 ppm (Figure 1). This leaves the ca. twice as intense -111 ppm resonance assigned to the other equivalent -CH₂-hydrogens.

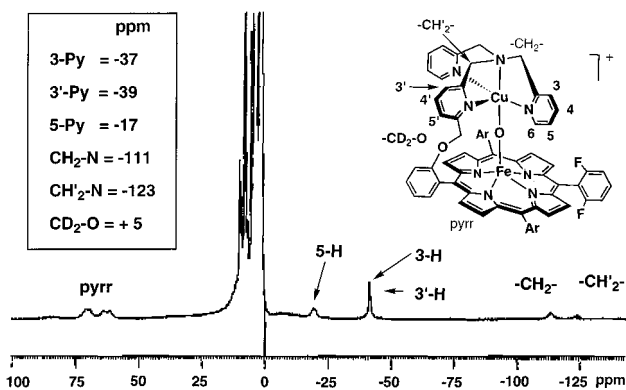


Figure 1. ^1H NMR spectrum of $[(^6\text{L})\text{Fe}^{\text{III}}-\text{O}-\text{Cu}^{\text{II}}]^+$ (**4**) in CD_3CN .

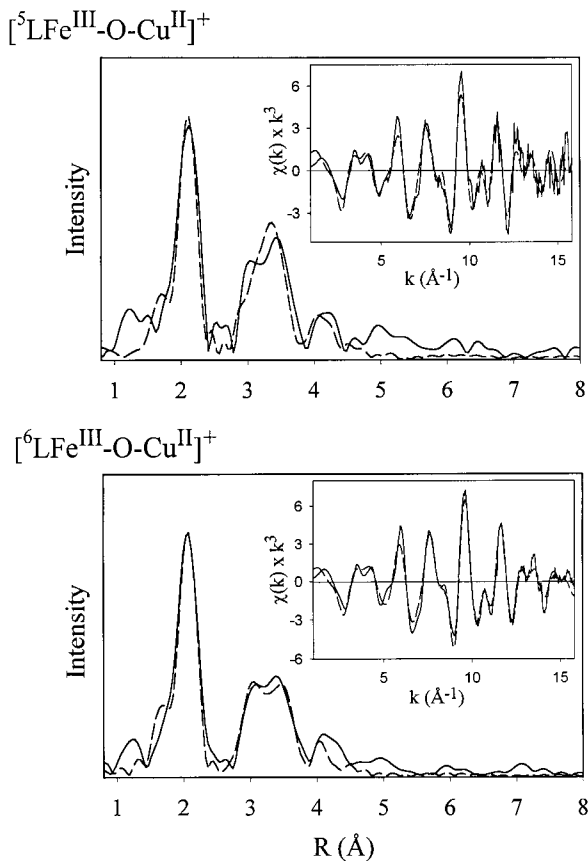


Figure 2. Experimental (solid line) versus simulated (dashed line) Fe K-EXAFS and Fourier transforms for **4** and **5**.

troscopy at both Fe (Figure 2) and Cu K-edges (Scheme 1, and Supporting Information).¹⁴ Both **4** and **5** exhibit the same extremely short Fe–O ($1.76 \text{ \AA}_{\text{ave}}$) and Cu–O (1.84 \AA) bond distances observed in **1** and seen elsewhere.¹⁵ However, varying ligand constraints in ^6L and ^5L impose dramatically different angular properties to the Fe–O–Cu moieties. Complex **1** has a linear bridging core ($\angle\text{Fe}-\text{O}-\text{Cu} = 178.2^\circ$), and we find that for $[(^6\text{L})\text{Fe}^{\text{III}}-\text{O}-\text{Cu}^{\text{II}}]^+$ (**4**), $\angle\text{Fe}-\text{O}-\text{Cu} \cong 177 \pm 8^\circ$ (ave, Fe and Cu edges);¹¹ 170.8° in the X-ray structure¹⁴), only slightly distorted from linearity. However, there is a severe contortion in $[(^5\text{L})\text{Fe}^{\text{III}}-\text{O}-\text{Cu}^{\text{II}}]^+$ (**5**), where $\angle\text{Fe}-\text{O}-\text{Cu} \cong 141 \pm 6^\circ$ (ave, Fe and Cu edges).¹¹

The structural variations in **4** and **5** manifest themselves in modulated physicochemical properties, also in comparison with the “parent” complex $[(\text{F}_8\text{-TPP})\text{Fe}^{\text{III}}-\text{O}-\text{Cu}^{\text{II}}(\text{TMPA})]^+$ (**1**). For example, we observed an oxygen isotope sensitive vibration using IR spectroscopy, $\nu(\text{Fe}-\text{O}-\text{Cu}) = 856 \text{ cm}^{-1}$ for **1**.¹² For **4** and **5**, the corresponding peaks are at 832 and 838 cm^{-1} , respectively.¹⁶ Examination of ^1H NMR temperature-dependent δ vs $1/T$ plots

are linear but exhibit obvious differences for **4** and **5** compared to that for **1**. For example, the slopes (reflecting proton sensitivity to unpaired spin density and Fe–Cu magnetic interactions) for pyrrole hydrogens (sensing iron) are similar for **4** and **5**, but differ significantly from that for **1**.¹² Together, these observations suggest that bending of the Fe–O–Cu moiety changes physical and chemical (vide infra) properties compared to the situation with linear geometry. The stability and basicity of the oxo-bridge in $[(^6\text{L})\text{Fe}^{\text{III}}-\text{O}-\text{Cu}^{\text{II}}]^+$ (**4**), $[(^5\text{L})\text{Fe}^{\text{III}}-\text{O}-\text{Cu}^{\text{II}}]^+$ (**5**), and $[(\text{F}_8\text{-TPP})\text{Fe}^{\text{III}}-\text{O}-\text{Cu}^{\text{II}}(\text{TMPA})]^+$ (**1**) also vary. We observe that **4** and **5** are much less stable to moisture and protic solvents than is **1** and the tethered ligands are more susceptible to protonation (Scheme 1). In CH_3CN solvent, addition of 1 equiv morpholinium triflate ($\text{p}K_{\text{a}} = 16.6$) does not cause protonation of **1** ($14 < \text{p}K_{\text{a}}(\text{2}) < 17$).^{9b} However, **4** reacts with this same acid to give a $\mu\text{-OH}^-$ species formulated as $[(^6\text{L})\text{Fe}^{\text{III}}-\text{OH}-\text{Cu}^{\text{II}}]^{2+}$, with characteristic pyrrole resonances at 72 and 76 ppm, which are similar to that in **2**, but distinct from data on $\mu\text{-oxo}$ complex **4** ($\delta = \sim 65$ ppm), or high-spin (porphyrinate)- $\text{Fe}^{\text{III}}-\text{OH}$ species ($\delta = 80\text{--}81$ ppm) where the bridge has broken. In fact, the latter is what occurs for the protonation of **5**. The results indicate that the $\mu\text{-oxo}$ atom in **4** and **5** is more basic than that in **1**, and a $\mu\text{-OH}^-$ complex appears inaccessible in **5**. With the stronger acid *N*-methylmorpholinium triflate ($\text{p}K_{\text{a}} = 15.6$), all three complexes react, again affording $\mu\text{-OH}^-$ products for **1** (to give complex **2**) and **4** (Scheme 1), but bridge breaking occurs again from reaction with **5**. Compared to **1**, the $\mu\text{-oxo}$ ligand in **4** is more basic by ~ 1 $\text{p}K_{\text{a}}$ unit, with that in **5** possibly even greater. The basicity of O_2 -derived reduced intermediates (e.g., peroxy, ferryl, oxo, and hydroxo) may be critical to the proton-translocating heme-copper oxidase function.^{2,7}

In conclusion, use of the new binucleating ligands ^5L and ^6L shows the utility of the synthetic model approach in the design and generation of new complexes which allow further elucidation of heme-copper structure, physicochemical and spectroscopic correlations, and functional chemistry. Here, we have shown that variations in the ligand architecture produce small yet significant changes in the metal environment (analogous to protein-enforced active-site geometric relationships) which in turn significantly influence structure and reactivity. Notably, we have characterized new $\mu\text{-oxo}$ Fe–O–Cu complexes with typically short M–O bonds, but provide the first example (**5**) with a remarkably bent configuration. The accompanying $\mu\text{-oxo}$ group proton uptake chemistry is significantly influenced, further demonstrating the importance of subtle ligand environment effects upon the structure and chemistry of the Fe–X–Cu core. While protein EXAFS data preclude the presence of an isolable enzyme form having a near-linear Fe–O–Cu moiety,^{9b,17} the present results demonstrate the plausible existence of a bent analogue, with enhanced proton affinity, possibly relevant to enzyme function. Further detailed characterization of the chemistry of **4** and **5**, including that of reduced derivatives and their O_2 -reactivity, is planned.

Acknowledgment. We thank the National Institutes of Health (K.D.K., GM 28962; N.J.B., GM 54803) for research support.

Supporting Information Available: Figures S1 with Cu K-EXAFS and Fourier transforms for **4** and **5**, Table 1 with EXAFS refinement results, EXAFS experimental details, and synthetic details (with Schemes S1 and S2) (12 pages). See any current masthead page for ordering information and Web access instructions.

JA9810989

(14) An X-ray crystal structure (to be published elsewhere) corroborates XAS derived structural results for **4**.

(15) Lee, S. C.; Holm, R. H. *J. Am. Chem. Soc.* **1993**, *115*, 11789–11798.

(16) Future studies will be required to deduce correlations of vibrational spectroscopy and structure (e.g., $\angle\text{Fe}-\text{O}-\text{Cu}$) for this unsymmetrical Fe–O–Cu moiety. These may be quite complex, and there are a few examples, by comparison to non-heme Fe–O–Fe systems. For latter correlations, see for example, Sanders-Loehr, J.; Wheeler, W. D.; Shiemke, A. K.; Averill, B. A.; Loehr, T. M., *J. Am. Chem. Soc.* **1989**, *111*, 8084.

(17) Fann, Y. C.; Ahmed, I.; Blackburn, N. J.; Boswell, J. S.; Verkhovskaya, M. L.; Hoffman, B. M.; Wikström, M. *Biochemistry* **1995**, *34*, 10245–10255.